AJNR

Gradient Echo (GRASS) MR Imaging in Cervical Radiculopathy

Mary C. Hedberg, Burton P. Drayer, Richard A. Flom, John A. Hodak and C. Roger Bird

AJNR Am J Neuroradiol 1988, 9 (1) 145-151
http://www.ajnr.org/content/9/1/145

Gradient Echo (GRASS) MR Imaging in Cervical Radiculopathy

Mary C. Hedberg[1]
Burton P. Drayer
Richard A. Flom
John A. Hodak
C. Roger Bird

Limited flip angle (LFA), gradient echo imaging was performed in 130 patients for evaluation of cervical radicular complaints. The LFA study was compared with myelography, CT myelography, and surgical results. Image quality was considered good or excellent for 128 patients. The use of a 10° flip angle with a TR of 75 msec and TE of 12.3 msec consistently provided good contrast and signal-to-noise ratio, giving a CT myelographic effect. The use of both axial and sagittal LFA images was important for optimal detection of extradural defects and for distinction of herniated disk versus osteophyte. There was excellent correlation between the MR and surgical findings.

Our results suggest that MR imaging is the initial procedure of choice for the evaluation of suspected cervical radiculopathy.

Myelography and CT have been the standard methods for demonstrating degenerative spondylosis and herniated disks. The complications and patient discomfort inherent in intrathecal injection of contrast medium and subsequent imaging are well established [1–7]. MR imaging of the cervical spine is being used with increasing frequency to study these patients [8–11]. In most patients with clinically significant findings, however, myelography and CT are often performed after MR imaging and before surgery. New limited flip angle (LFA) MR imaging techniques in such patients may obviate the need for myelography and CT in making a diagnosis and meticulously delineating anatomy preoperatively [12–14]. High-resolution imaging of the cervical spine in the axial and sagittal planes with clear distinction of bony and disk margins, neural foramina, nerve roots, CSF, and spinal cord can be achieved with recently developed gradient recalled acquisition in the steady state (GRASS) techniques [12]. Another advantage of LFA imaging is rapid data acquisition, which improves the clinical efficiency of the examination and minimizes patient discomfort and motion.

Subjects and Methods

One hundred and thirty consecutive patients with known or suspected cervical radiculopathy were studied with MR LFA techniques between August 1986 and December 1986 with a 1.5-T GE Signa MR system. Imaging parameters included 5-mm-thick sections, contiguous imaging, 128 × 256 acquisition matrix, 24-cm field of view, four excitations (two averages), flip angle of 10° or 20°, TR = 75 msec, and TE = 12.3 msec. It generally required 16 sequential single axial sections to include the C3–T1 levels. LFA images were performed in the axial (n = 130) and sagittal (n = 75) planes. A flow compensation regimen (gradient moment nulling) was used with the GRASS sequences [12]. Image quality of the LFA studies was rated as poor, good, or excellent. T1-weighted (spin echo TR = 600, TE = 20 msec) and T2-weighted (spin echo TR = 2500, TE = 30 and 60 msec) sagittal images were also acquired. Myelography was done in 20 patients after intrathecal instillation of iopamidol (Isovue M-200 or 300).* CT myelography was performed after the cervical myelogram in 16 individuals. MR, CT, and conventional myelographic studies were divided into four groups depending on the dominant findings: (1) normal; (2) ventral extradural ridging, central; (3)

* Squibb, New Brunswick, NJ.

This article appears in the January/February 1988 issue of *AJNR* and the March 1988 issue of *AJR*.

Received June 29, 1987; accepted after revision September 2, 1987.

Presented at the annual meeting of the American Society of Neuroradiology, New York, May 1987.

[1] All authors: Department of Radiology and the Barrow Neurological Institute of St. Joseph's Hospital and Medical Center, 350 W. Thomas Rd., Phoenix, AZ 85013. Address reprint requests to B. P. Drayer.

***AJNR* 9:145–151, January/February 1988**
0195–6108/88/0901–0145

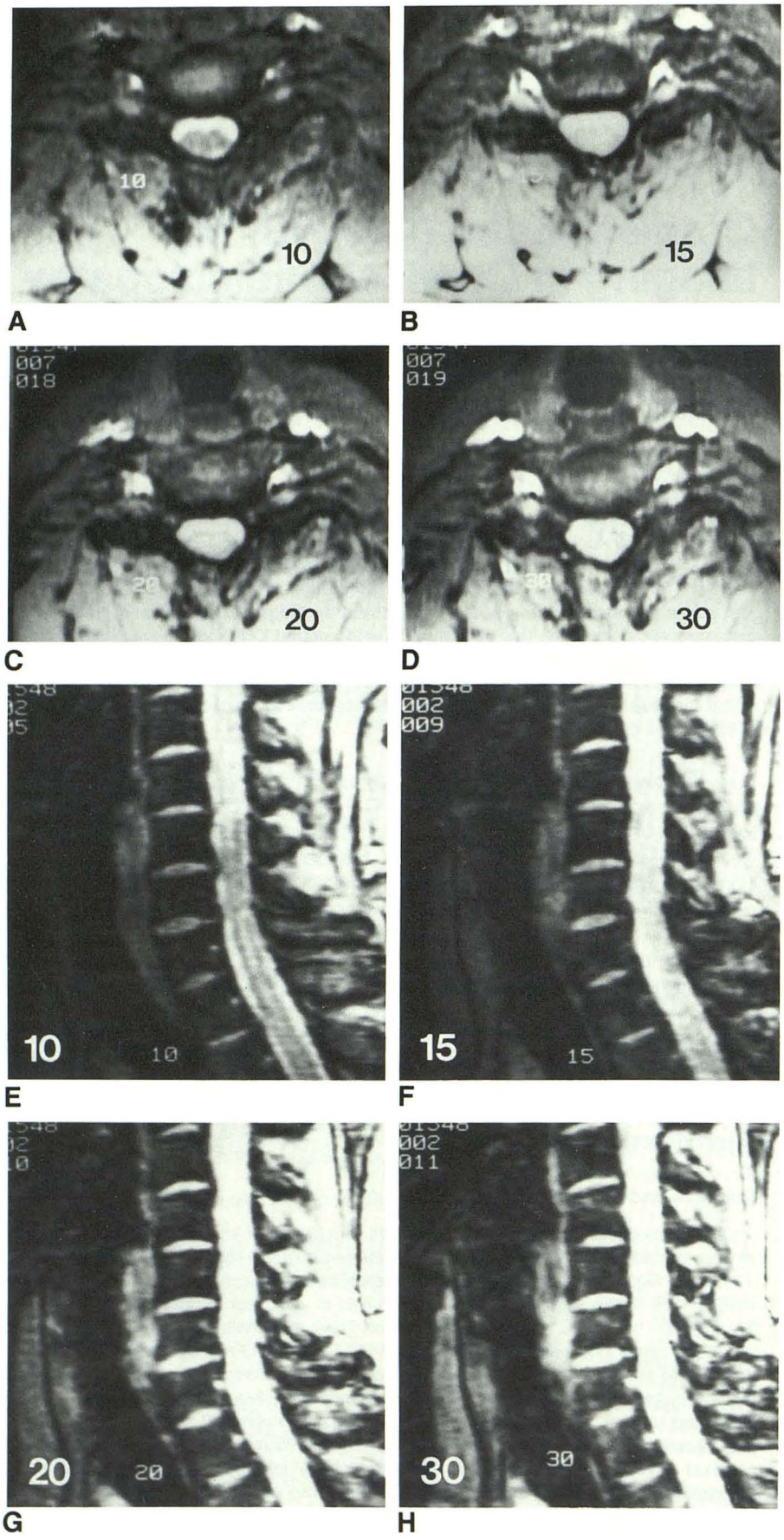

Fig. 1.—Optimizing flip angle for gradient echo imaging.

A–D, Axial MR images (TR = 75 msec, TE = 12.3 msec). TR and TE are held constant while flip angle is varied (10°, 15°, 20°, and 30°). Although signal-to-noise ratio is best at 30°, the contrast between spinal cord and surrounding CSF is best at 10°, and signal-to-noise is sufficient.

E–H, Sagittal MR images (TR = 75 msec, TE = 12.3 msec). Signal-to-noise ratio is again best at 30° but cord vs CSF contrast is best at 10° flip angle.

ventrolateral extradural, degenerative spurring; and (4) ventrolateral extradural, herniated disk. Pathologic confirmation of the diagnosis at surgery was obtained in 13 patients.

Results

Image quality, evaluated from the LFA images, was judged as excellent (n = 95), good (n = 33), or poor (n = 2). A 10° or 15° flip angle provided better image contrast of the spinal cord versus surrounding subarachnoid space than a 30° flip angle when using TR = 75 msec and TE = 12.3 msec (Fig. 1). The signal intensity of the CSF was greater than the spinal cord, similar in appearance to that seen with intrathecally enhanced CT scanning (Fig. 2). There was no significant CSF pulsation artifact. The central portion of the spinal cord was of higher signal intensity than the periphery on axial images, suggesting a distinction of central gray from surrounding white matter and/or truncation artifact because the shape does not precisely coincide with the anterior and posterior horns (Fig. 3). A thin central ribbon of high signal intensity was seen on the sagittal 128 × 256 matrix images of the spinal cord and was absent on 256 × 256 matrix images, consistent with truncation artifact [15]. The upper cervical cord and cervicomedullary junction were also visualized on the cervical studies. The neural foramina were routinely evident on axial studies and contained linear, lower signal intensity nerve roots (Fig. 3). The cervical vertebral bodies were of lower signal intensity than the intervening disks.

Thirty-one studies were judged normal. Neither surgery nor conventional or CT myelography was performed on these patients.

Extradural defects were apparent in 99 of 130 MR studies. Both conventional and CT myelography were performed in 20 patients, and five patients had nonenhanced CT with confirmation of the MR findings in all cases. The extradural defects, whether central or lateral, were clearly delineated due to compression of the neural foramina, nerve roots, and adjacent subarachnoid space. The distinction of osteophyte versus herniated disk material was apparent in the majority of cases (Table 1). Degenerative bony ridging was of lower signal intensity than disk material (Fig. 4). The herniated disk (Fig. 5) often created a smooth, lateralized compression of the subarachnoid space on the sagittal MR studies that resembled a double density on a lateral conventional myelographic study. Larger extradural defects resulted in spinal cord compression and often posterior displacement. The vertical band of increased signal intensity in the central spinal cord was focally lost with milder cord effacement from either bony ridge or herniated disk. The MR study always provided equivalent and, at times, additional information, compared

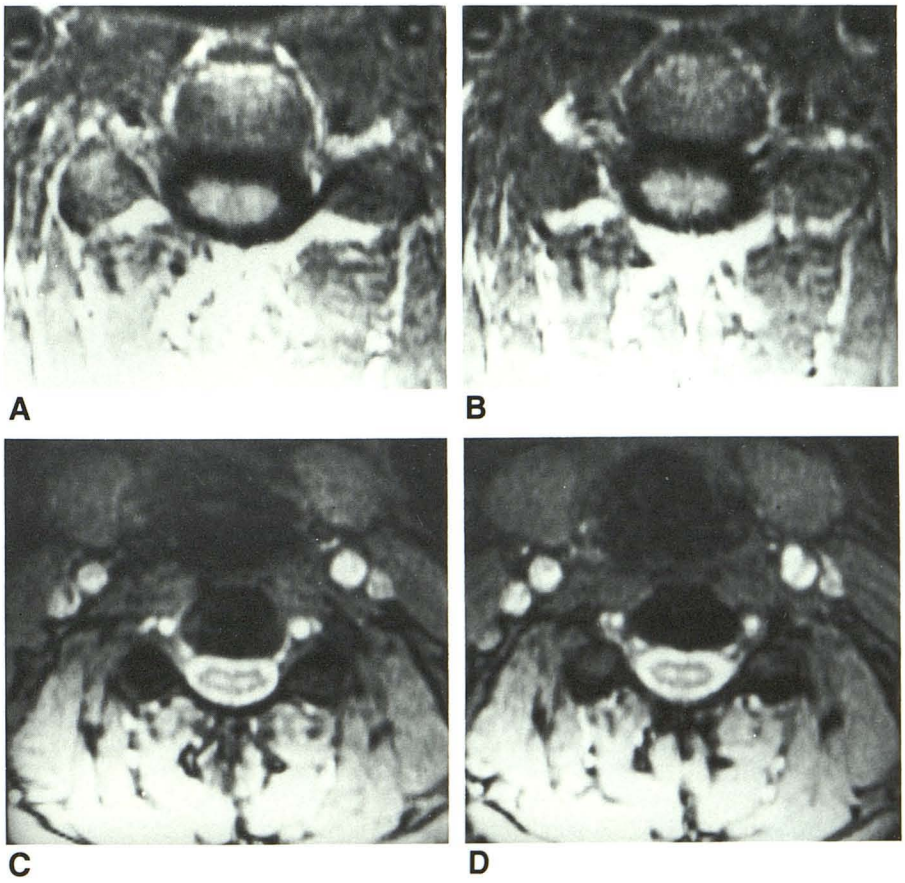

Fig. 2.—Spin echo vs GRASS images of cervical spine.

***A* and *B*, T1-weighted spin echo images (TR = 600 msec, TE = 20 msec) at C5–C6 level depict spinal cord excellently. Surrounding CSF is also well defined but extradural defects are difficult to visualize (e. g., both CSF and bony degenerative abnormalities are low signal intensity).**

***C* and *D*, Gradient echo (GRASS) images (TR = 75 msec, TE = 12.3 msec, flip angle at 10°) at same C5–C6 level clearly define spinal cord, surrounding CSF, neural foramina, and exiting C6 nerve roots. CT myelographic appearance improves the ability to readily differentiate normal from abnormal studies.**

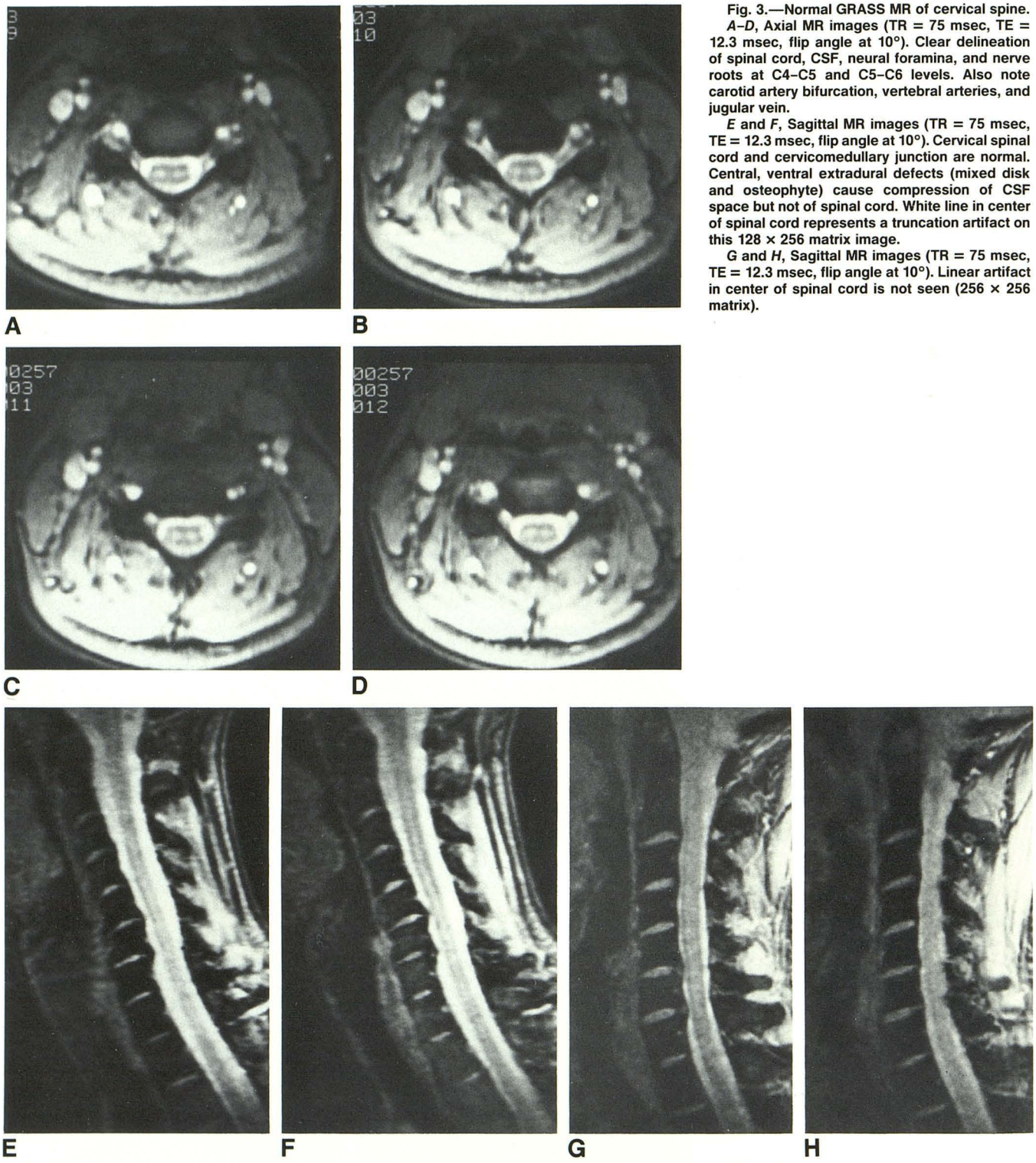

Fig. 3.—Normal GRASS MR of cervical spine.

A–D, Axial MR images (TR = 75 msec, TE = 12.3 msec, flip angle at 10°). Clear delineation of spinal cord, CSF, neural foramina, and nerve roots at C4–C5 and C5–C6 levels. Also note carotid artery bifurcation, vertebral arteries, and jugular vein.

E and *F*, Sagittal MR images (TR = 75 msec, TE = 12.3 msec, flip angle at 10°). Cervical spinal cord and cervicomedullary junction are normal. Central, ventral extradural defects (mixed disk and osteophyte) cause compression of CSF space but not of spinal cord. White line in center of spinal cord represents a truncation artifact on this 128 × 256 matrix image.

G and *H*, Sagittal MR images (TR = 75 msec, TE = 12.3 msec, flip angle at 10°). Linear artifact in center of spinal cord is not seen (256 × 256 matrix).

with myelography and CT. A subtle, but definite sign of an extradural defect on the axial images was loss of the increased signal intensity CSF anterior to the spinal cord. The anterior CSF space and the space posterior to the spinal cord should be similar in size, creating an oblong shape of equal thickness (Figs. 2 and 3). The correlation of surgical pathology and the GRASS MR findings was excellent (Table 2). There was lack of correlation only at the level where the bony

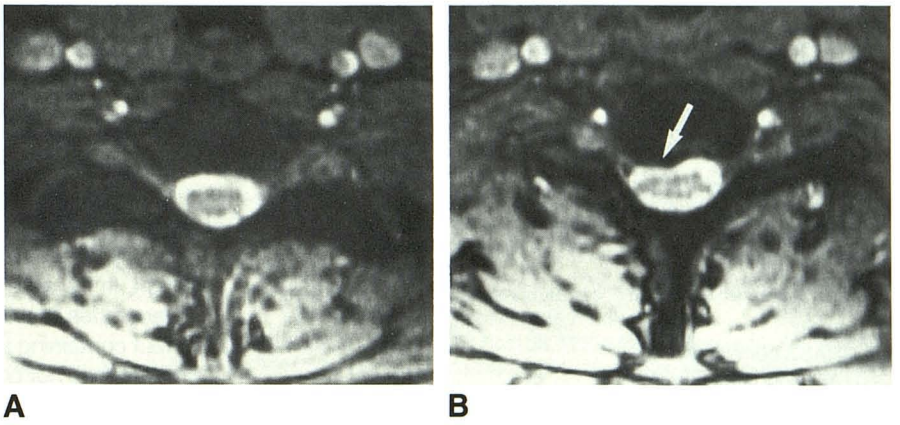

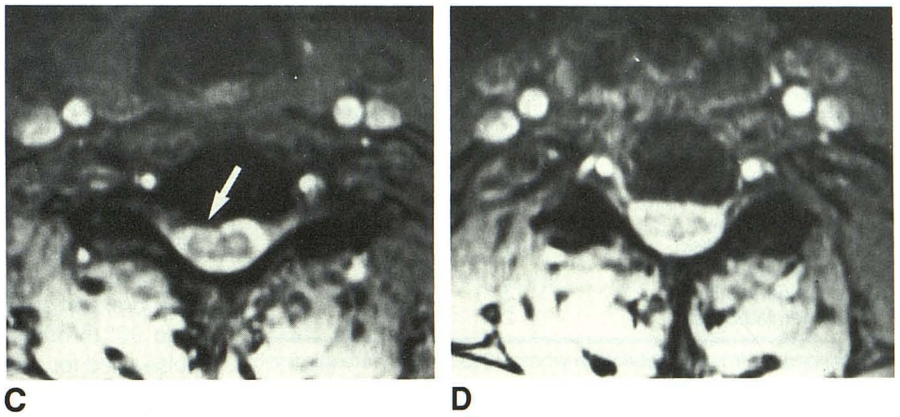

Fig. 4.—Ventrolateral extradural defect, C7 radiculopathy. GRASS images (TR = 75 msec, TE = 12.3 msec, flip angle at 10°) at C7–T1 (*A*), C6–C7 (*B* and *C*), and C5–C6 levels (*D*). Prominent ventrolateral extradural defect (*arrow*) on right at C6–C7 level causes compression of subarachnoid space, neural foramen, and C7 nerve root. Extradural defect is of mixed low and intermediate signal intensity, consistent with hard and soft disk material, respectively. Characterization of degenerative bony versus herniated disk material often requires sagittal image information due to partial volume averaging effects.

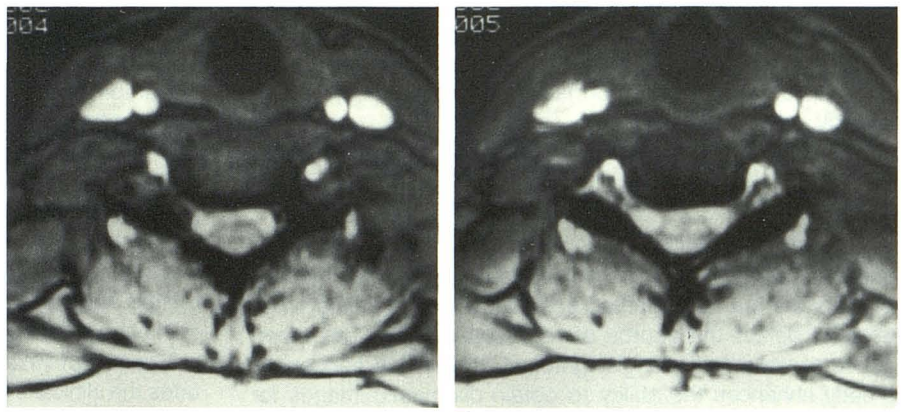

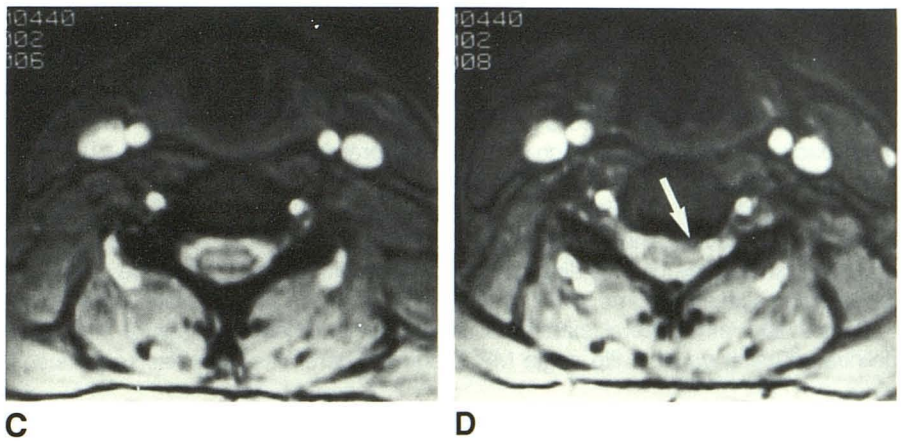

Fig. 5.—Herniated cervical disk. GRASS images (TR = 75 msec, TE = 12.3 msec, flip angle at 10°) at C6–C7 levels (*A* and *B*) and at C5–C6 levels (*C* and *D*). A small herniated disk (*arrow*) is present on the left at C5–C6 level, causing compression of subarachnoid space but not of the neural foramen. The intermediate signal intensity distinguishes this soft disk from uncovertebral spurring.

TABLE 1: GRASS MR Imaging in Cervical Radiculopathy

A. Diagnosis
Normal ($n = 31$)
Extradural defects ($n = 99$)
Central, ventral (52)
Ventrolateral
Degenerative (osteophyte) (26)
Herniated disk (4)
Degenerative/herniated (17)
B. Imaging quality
Excellent (95)
Good (33)
Poor (2)
C. GRASS correlation
CT/myelography (25/25)
Surgical (13/13)

TABLE 2: GRASS/Surgical Pathology Correlation[a]

	Surgical Pathology	GRASS Correlation
Ventral extradural		
Degenerative	15	15
Herniated disk	1	1
Ventrolateral extradural		
Degenerative	12	11
Herniated disk	2	2

[a] Results are from 13 patients in whom 30 locations were surgically explored.

degenerative abnormality on the MR study was more prominent on the right, while surgery was performed on the left (the side of milder MR abnormality) due to clinical symptomatology.

Conclusions

Conventional spin echo imaging paradigms have provided excellent delineation of the spinal cord for the evaluation of myelopathy but have proved somewhat disappointing when used to detect the source of radiculopathy [9]. The emergence of variable flip angle, gradient echo pulse sequences greatly enhances the ability to obtain diagnostic images for the clinical evaluation of cervical radiculopathy. The major advantage of the variable flip angle, gradient echo method (compared with spin echo sequences) becomes most apparent when imaging the cervical spine in the axial plane. There is sharp delineation of bone and disk margins, excellent contrast between the spinal cord and surrounding subarachnoid space, and clear visualization of the neural foramina and exiting nerve roots. The visual effect of these noninvasive MR images is similar to that of intrathecally enhanced CT (CT myelographic effect). The gradient echo technique has the additional advantage of providing good signal-to-noise ratio with a short acquisition time [12].

Central and ventrolateral extradural defects were readily delineated using variable flip angle MR imaging. There was clear distinction of nerve roots, neural foramina, and spinal cord impingement. Surgical correlation with the gradient echo images was excellent. The MR studies gave equal or more detailed information compared with myelography/CT in all cases in which both were performed.

Degenerative bony ridging was of lower signal intensity than herniated disk material. This distinction was often difficult using axial, 5-mm sections, and it is thus critical to analyze carefully both axial and sagittal images to make this differentiation. In 17 cases we were unable to definitely differentiate osteophytes and disk material, generally due to the extradural defect containing a mixture of both. Larger extradural defects compressed not only the subarachnoid space and nerve roots but also displaced the spinal cord. Subtle cord effacement resulted in loss of the central cord region high signal intensity. This high signal intensity is related to a truncation artifact [15] that is seen with a 128 × 256 acquisition matrix, but not with a 256 × 256 matrix. It is also important to recognize that even mild to moderate effacement of the anterior subarachnoid space on axial images is diagnostic of an extradural defect.

The limited flip angle MR images were obtained with a GRASS pulse sequence and gradient moment nulling (flow compensation) to eliminate signal loss from motion-induced temporal and spatial phase shift [12]. Pulse flip angles of less than 90° produce a greater signal than the traditional 90° pulse used for spin echo imaging, particularly when used with a short TR. The shorter flip angle is followed by a negative gradient in the readout direction causing dephasing of spins and then a positive gradient causing rephasing [12]. By obtaining a series of images with a TR of 75 msec and TE of 12.3 msec, we empirically determined that even though the signal-to-noise ratio was greatest with a 30° flip angle the contrast between the spinal cord and surrounding subarachnoid space was greatest at a 10° flip angle. We chose a TR of 75 msec for a better signal and because a shorter TR (e.g., TR-25 msec) sequence was extremely uncomfortable (loud gradient knocking) for the patient. Imaging contrast and relative relaxation time weighting in GRASS imaging are thus related not only to the operator-selected TR and TE, as with spin echo imaging, but also to pulse flip angle.

The use of limited flip angle GRASS imaging greatly facilitates the clinical evaluation of cervical radiculopathy. A routine cervical study can now be performed in 21 min, 53 sec using the following pulse sequences: (1) sagittal multislice spin echo, TR = 600 msec, TE = 20 msec, 256 × 256 matrix, two excitations; (2) sagittal GRASS, TR = 75 msec, TE = 12.3 msec, flip angle 10°, 256 × 256 matrix, four excitations, 5 slices; and (3) axial GRASS, TR = 75 msec, TE = 12.3 msec, flip angle 10°, 128 × 256 matrix, four excitations, 24-cm field of view, and approximately 16 slices (C3–T1). All images are flow compensated, and contiguous 5-mm-thick (0 skip) sections are used. The major limitation of the GRASS images is that they provide suboptimal visualization of spinal cord disease. In patients presenting with myelopathy an additional sagittal multislice, multiecho, flow compensated spin echo pulse sequence (TR = 2000 msec, TE = 35/70 msec, 128 ×

256 matrix, two excitations) is performed. This study suggests that MR imaging may obviate the need for the more invasive myelography and CT scanning in individuals with suspected cervical radiculopathy.

ACKNOWLEDGMENTS

We appreciate the superb technical assistance of MR technologists James Winters, Kevin King, Linnea Tyman, and Laura Castillo.

REFERENCES

1. Drayer BP, Rosenbaum AE. Metrizamide brain penetrance. *Acta Radiol [Suppl] (Stockh)* **1977**;355:280–293
2. Sykes RHD, Wasenaar W, Clark P. Incidence of adverse effects following metrizamide myelography in nonambulatory and ambulatory patients. *Radiology* **1981**;138:625–627
3. Hauge O, Falkenberg H. Neuropsychological reactions and other side effects after metrizamide myelography. *AJR* **1982**;139:357–360
4. Davis CE Jr, Smith C, Harris R. Persistent movement disorder following metrizamide myelography. *Radiology* **1982**;144:A975
5. Killebrew K, Whaley RA, Hayward JN, Scatliff JH. Complications of metrizamide myelography. *Radiology* **1983**;149:A343
6. Meador K, Hamilton WJ, El Gammal TAM, Demetropoulos KC, Nichols FT. Irreversible neurologic complications of metrizamide myelography. *Radiology* **1985**;154:A564
7. Drayer BP, Vassallo C, Sudilovsky A, et al. A double-blind clinical trial of iopamidol versus metrizamide for lumbosacral myelography. *J Neurosurg* **1983**;58:531–537
8. Modic MT, Weinstein MA, Pavlicek W, Boumphrey F, Starnes D, Duchesneau PM. Magnetic resonance imaging of the cervical spine: technical and clinical observations. *AJR* **1983**;141:1129–1136, *AJNR* **1984**;5:15–22
9. Modic MT, Masaryk TJ, Mulopulos GP, Bundschun CV, Han JS, Bohlman H. Cervical radiculopathy; prospective evaluation with surface coil MR imaging; CT with metrizamide and metrizamide myelography. *Radiology* **1986**;161:753–759
10. Daniels DL, Hyde JS, Kneeland JB, et al. The cervical nerves and foramina: local-coil MR imaging. *AJNR* **1986**;7:129–133
11. Modic MT, Masaryk TJ, Ross JS, Mulopulos GP, Bundschun CV, Bohlman H. Cervical radiculopathy: value of oblique MR imaging. *Radiology* **1987**;163:227–231
12. Wehrli FW, Shimakawa A, Gullberg GT, MacFall JR. Time-of-flight MR flow imaging: selective saturation recovery with gradient refocusing. *Radiology* **1986**;160:781–785
13. Perkins TG, Wehrli FW. CSF signal enhancement in short TR gradient echo images. *Magn Reson Imaging* **1986**;4:465–467
14. Enzmann DR, Rubin JB, Wright A. Cervical spine MR imaging: Generating high signal CSF in sagittal and axial images. *Radiology* **1987**;163:233–238
15. Wood ML, Henkelman RM. Truncation artifacts in magnetic resonance imaging. *Mag Reson Med* **1985**;2(6):517–526